DOI:10.1021/jf900932h

JOURNAL OF AGRICULTURAL AND FOOD CHEMISTRY
ARTICLE

Identification of Hydroxycinnamic Acid−Maillard Reaction Products in Low-Moisture Baking Model Systems

Deshou Jiang,[†] Christopher Chiaro,[§] Pranav Maddali,[§] K. Sandeep Prabhu,[§] and Devin G. Peterson*,[†]

[†]Department of Food Science and Nutrition, 147 FScN Building, The University of Minnesota, St. Paul, Minnesota 55108, and [§]Department of Veterinary and Biomedical Sciences, The Pennsylvania State University, University Park, Pennsylvania 16802-2504

The chemistry and fate of hydroxycinnamic acids (ferulic, *p*-coumeric, caffeic, sinapic, and cinnamic acid) in a glucose/glycine simulated baking model (10% moisture at 200 °C for 15 min) were investigated. Liquid chromatography−mass spectrometry analysis of glucose/glycine and glucose/glycine/hydroxycinnamic acid model systems confirmed the phenolics reacted with Maillard intermediates; two main reaction product adducts were reported. On the basis of isotopomeric analysis, LC-MS, and NMR spectroscopy, structures of two ferulic acid−Maillard reaction products were identified as 6-(4-hydroxy-3-methoxyphenyl)-5-(hydroxymethyl)-8-oxabicyclo[3.2.1]-oct-3-en-2-one (adduct **I**) and 2-(6-(furan-2-yl)-7-(4-hydroxy-3-methoxyphenyl)-1-methyl-3-oxo-2,5-diazabicyclo[2.2.2]oct-5-en-2-yl)acetic acid (adduct **II**). In addition, a pyrazinone-type Maillard product, 2-(5-(furan-2-yl)-6-methyl-2-oxopyrazin-1(2*H*)-yl) acetic acid (**IIa**), was identified as an intermediate for reaction product adduct **II**, whereas 3-deoxy-2-hexosulose was identified as an intermediate of adduct **I**. Both adducts **I** and **II** were suggested to be generated by pericyclic reaction mechanisms. Quantitative gas chromatography (GC) analysis and liquid chromatography (LC) also indicated that the addition of ferulic acid to a glucose/glycine model significantly reduced the generation of select Maillard-type aroma compounds, such as furfurals, methylpyrazines, 2-acetylfuran, 2-acetylpyridine, 2-acetylpyrrole, and cyclotene as well as inhibited color development in these Maillard models. In addition, adducts **I** and **II** suppressed the bacterial lipopolysaccharide (LPS)-mediated expression of two prototypical pro-inflammatory genes, inducible nitric oxide synthase (iNOS) and cyclooxygenase (COX)-2, in an in vitro murine macrophage model; ferulic acid reported negligible activity.

KEYWORDS: Hydroxycinnamic acids; Maillard reaction; pericyclic reaction; iNOS and COX-2 suppression; Maillard−phenolic reaction product

INTRODUCTION

Whole grain foods are considered to be a key component of a healthy diet. The 2005 U.S. Department of Agriculture dietary guidelines recommend at least three servings of whole grain foods daily. These recommendations are based on the increasing number of epidemiological studies supporting the conclusion that whole grain consumption can reduce the risk of several chronic diseases, such as cardiovascular disease, diabetes, and cancer, and may help with weight maintenance (*1*).

The manufacture of whole grain foods can be challenging as limited information is known about the compounds that affect health promotion and likewise limit strategies for process optimization. Furthermore, although whole grain products have a perceived positive health benefit among consumers, changes in the flavor properties can be viewed negatively and ultimately influence product choice. Bakke and Vickers (*2*) reported people preferred refined grain bread to whole grain bread when both were made with equivalent ingredients (refined versus whole grain flour). The negative flavor properties of whole grain foods have been related to the bitter taste properties of the intrinsic phenolic compounds (*3*). Food phenolics are commonly considered to negatively contribute to the flavor attributes of foods (*4*).

The hydroxycinnamic acid phenolic compounds in whole grain foods are considered to be, in part, bioactives involved in health promotion and largely related to antioxidant function (*1*). Hydroxycinnamic acids have also been reported to influence the Maillard-type aroma development in model and food systems and therefore may relate to negative changes in the flavor properties of whole grain foods in comparison to refined grain products. Peterson and Noda (*5*) reported ferulic acid was reactive in aqueous glucose/glycine model system generated adducts with Maillard intermediates (sugar fragments and sugar fragments with a glycine moiety) and likewise suppressed the generation of Maillard-type aroma compounds. Wang (*6*) indicated that hydroxycinnamic acids can inhibit the formation of

*Author to whom correspondence should addressed [e-mail dgp@umn.edu; telephone (612) 624-3201; fax (612) 625-5272].

 Published on Web 10/09/2009

aroma compounds in coffee model systems consisting of leucine, lysine, or cysteine with glucose. Wang suggested that hydroxycinnamic acids, as antioxidants, altered Maillard chemistry by scavenging Maillard-type reactive radical precursors (i.e., dialkylpyrazine radical) and thereby suppressed Maillard product generation.

Hydroxycinnamic acids (HCAs) are widely distributed in plant-based food products either in free form or associated with other component polysaccharides (*7*). Understanding the chemistry and fate of the hydroxycinnamic acids in processed foods as affected by food reactions such as the Maillard reaction may provide insights into whole grain food chemistry in relation to health promotion and flavor development. The Maillard reaction, a key food reaction, is known to affect food flavor, color, toxicity, and nutritional value and is considered to play an important role in regulatory biology and age-related pathology (*8*−*12*). Consequently, the hydroxycinnamic acids could affect the quality of whole grain foods by modifying the composition of the Maillard products generated as well as by the generation of other bioactive phenolic-containing reaction products during processing. Others have reported thermal processing influenced the health-relevant functionality in grain sprouts and seedlings (*13*).

Baking is a common processing technology for making whole grain foods. The objectives of this study were to investigate the reactivity of the free hydroxycinnamic acids in a low-moisture glucose/glycine simulated model baking system on the generation of Maillard-type reaction products and on the bioactivity of related Maillard degraded phenolic compounds as seen with their ability to modulate expression of two prototypical pro-inflammatory genes in an in vitro macrophage model.

MATERIALS AND METHODS

Chemicals. D-Glucose, glycine, D-[$^{13}C_6$]glucose (99% enrichment), high-purity quartz sand, formic acid, 2,5-dimethylpyrazine, 5-hydroxymethylfurfural, 2-acetylpyrrole, 2-acetylpyridine, 2,3,5-trimethylpyrazine, 5-methylfurfural, 2-acetylfuran, furfural, 2-methyl-3-heptanone, 3-methyl-1,2-cyclopentanedione, [^{15}N,$^{13}C_2$]glycine (99% enrichment), methanol-d_4 (99.8% enrichment), and DMSO-d_6 were obtained from Sigma Aldrich Co. (St. Louis, MO). Ferulic acid was obtained from MP Biomedicals (Aurora, OH), and 2-methoxy-4-vinylphenol was purchased from Alfa Aesar (Heysham, Lancaster, U.K.). High-performance liquid chromatography (HPLC) grade methanol was obtained from EMD Chemicals (Gibbstown, NJ). 3-Deoxy-2-hexosulose was purchased from Toronto Research Chemicals (Ontario, Canada).

Low-Moisture Baking Reaction Model. Reactions were conducted according to those of Wang (*6*). In brief, the reaction apparatus consisted of a round-bottom flask (500 mL) attached with a Vigreux column and a glass stirrer fitted with a Teflon blade (Ace Glass, Vineland, NJ). The reaction vessel was heated with an oil bath connected to a rheostat (PowerStat, The Superior Electric Co., Bristol, CT) for temperature control. The reactants (reported in **Table 1**) were mixed with 15 g of quartz sand (previously cleaned and dried) and 1.5 g of water. The reactant mixture was mixed at 40−60 rpm in the round-bottom flask for 2−3 min. The apparatus was then placed in an oil bath maintained at 200 °C, and the reaction was conducted for 15 min, immediately removed from the oil bath, and prepared for further analysis.

Sample Preparation for Gas Chromatography (GC) Analysis. The reaction mixture was extracted (3 × 30 mL) with diethyl ether spiked with internal standard 2-methyl-3-heptanone (1 μL/2000 mL), filtered, and subsequently concentrated to 0.5 mL by spinning band distillation (model 800, B/R Instruments, Easton, MD) prior to GC and gas chromatography−mass spectrometry (GC-MS) analysis.

GC-MS. The extracts were analyzed by an Agilent 6890 gas chromatograph connected to an Agilent 5973 mass spectrometer operating in EI mode (Agilent Technologies, Palo Alto, CA). Sample introduction was performed using a liquid autosampler (A200SE, CTC Analytics, Carrboro, NC). All analyses were performed on DB-5 MS capillary columns (Agilent Technologies; 30 m × 0.25 mm i.d. with a 0.25 μm film thickness). The analysis parameters were as follows: 1 μL of sample was injected in splitless mode, the inlet temperature was 200 °C, and the column flow was constant at 1.0 mL/min (helium). The temperature program was 35 °C for 2 min, ramped at 3 °C/min to 250 °C, and held for 4 min. The MSD operational parameters were as follows: capillary direct interface temperature at 250 °C, source temperature at 150 °C, and mass range of 35−250 amu at 6.35 cycles/min. Positive identifications by GC-MS were determined by comparing the mass spectra fragmentation pattern of analytes with mass spectra of known compounds from the Wiley Database and authentic compounds. Linear retention index values were calculated using an *n*-alkane ladder.

Sample Preparation for LC-MS Analysis. The reaction materials were extracted with 100 mL of methanol for 30 min, filtered, and evaporated until dryness under vacuum (Buchi Rotavapor, model R110, New Castle, DE; 0.1 atm, water bath was maintained at 30 °C), and the residue was re-extacted with 3 mL of 10% methanol aqueous solution. A 1 g C18 Sep-Pak cartridge (Supelco, Bellefonte, PA) was preconditioned with methanol (3 mL) and nanopure water (5 mL). The 3 mL reaction mixture extract was loaded (1 mL/min) over the preactivated Sep-Pak cartridge, washed with 5 mL of nanopure water, and then eluted with 2 mL of methanol. The isolate was subsequently filtered through a 0.45 μm PTFE tip filter (Sigma Aldrich Co.) using a 1 mL syringe (Millipore, Bedford, MA) and analyzed by LC-MS.

LC-MS/MS-ESI. Sample analysis was conducted with a Shimadzu HPLC system (Shimadzu, Columbia, MD) coupled with a Waters triple-quadrupole mass spectrometer (Quattro Micro, Waters, Milford, MA) equipped with an electrospray ionization (ESI) probe. The HPLC system consisted of a binary pumping system (LC-10 ADvp), a degasser (DGU-14A), an autosampler (SIL-10vp), a water column heater (TCM model, Waters), a variable-wavelength UV−vis detector 280 nm) (Shimadzu, SPD-10a), and a reverse phase C-18 column (2.1 mm × 250 mm, 5 μm packing column, Ultra Aqueous C-18 column). Ten microliters of the extracts was injected on the RP-18 column maintained at a temperature of 25 °C using a binary solvent system of 0.1% formic acid (A) and methanol (B). The mobile phase consisted of a series of linear gradients of B in A starting at 10% B in A (0−2 min), increasing to 90% B in A (2−30 min), then held at 90% for 5 min (30−35 min), and then decreasing to 10% B in A (35−37 min). Mass spectrometric ionization conditions were as follows: desolvation temperature, 300 °C; source temperature, 110 °C; capillary voltage, 3.5 kV. For samples analyzed in scan mode the scan

Table 1. Low-Moisture Baking Model Reactions[a]

	reactant concn (mM)								
reactant	model A	model B	model C	model D	model E	model F	model G	model H	model I
glucose	3	3	1.5	3	3		3	3	
glycine	3	3	3	1.5			1.5	3	
3-DG						0.3			
ferulic acid		3	3	3	3				3
2-methoxy-4-vinylphenol						0.3		1	
[$^{13}C_6$]glucose			1.5						
[$^{13}C_2$,^{15}N]glycine				1.5					
[$^{13}C_2$]glycine							1.5		

[a] Reactants added to 15 g of quartz sand and 1.5 g of water and mixed at 40−60 rpm in a round-bottom flask at 200 °C for 15 min.

range was 80−1000 Da, whereas for sibling ion analysis, the CID was 3.4e−4, collision voltage was 21 V, and the sibling ions were scanned over a range of m/z 20−500.

Select precursors and reaction products were quantified by tandem MS techniques. The amounts of ferulic acid, adduct **I**, and adduct **II** were quantified by the peak areas determined by MRM scanning (ferulic acid 178←193, adduct **I** 203 ← 275, adduct **II** 233 ← 383) with those of defined standard solution of the authentic reference compound in methanol. The amount of 2-methoxy-4-vinylphenol was quantified by the peak areas determined at λ = 254 nm with those of defined standard solution of the authentic reference compound in methanol.

LC-MS/Qtof-ESI. Accurate mass analysis was conducted with the same Shimadzu HPLC system (Shimadzu, Columbia, MD) described above coupled with a Waters Qtof mass spectrometer (Q-TOF micro) equipped with an electrospray ionization (ESI) probe and lock spray inlet system. Highly accurate mass acquisition of the ion of interest was performed by chromatography injection with reserpine as internal standard. Ten microliter injections of the extracts were injected on the RP-18 column maintained at a temperature of 25 °C using the same eluting condition as before. Mass spectrometric ionization conditions were as follows: desolvation temperature, 300 °C; source temperature, 100 °C; capillary voltage, 2.2 kV. For samples analyzed in scan mode the scan range was 80−1000 Da.

NMR Sample Preparation and Analysis. For adduct **I**, optimal conditions for sample purification were as follows: 30 mmol of glucose, 3 mmol of glycine, and 3 mmol of ferulic acid were reacted using the model reaction conditions described above. On the basis of LC-MS/UV analysis, the yield of adduct **I** at this reagent ratio was increased by nearly 23-fold compared to its yield at their original ratio (glucose/glycine/ferulic acid = 3:3:3). The reaction mixture was separated into ethyl acetate phase and aqueous phase (30 mL:30 mL). The organic phase was evaporated to dryness, and the residue was dissolved in 2 mL of the 50% methanol aqueous solution. The methanolic extract was filtered using a PTFE tip filter (0.45 μm) and further fractionated by LC-MS (instrument configuration was the same as described above) utilizing FractionLynx software (Waters Corp.) and a Waters Fraction Collector (III). One hundred microliters of the methanol extracted was fractionated using a Pursuit C-18 column maintained at 25 °C using a binary solvent system of 0.1% formic acid (A) and methanol (B) using a series of linear gradients of B in A starting at 10% B in A (0−3 min), increasing to 60% B in A (3−25 min), then increasing to 90% B in A (25−27 min), and then held at 90% for 3 min (27−30 min), decreasing to 10% B in A (30−32 min), and held at 10% for 6 min (32−38 min). Two peaks with an m/z 275 $[M-1]^-$, which were 0.5 min apart in retention time (see **Figure 5b**), were collected over approximately 30 independent injections, subsequently pooled, frozen at −20 °C, and then freeze-dried with a Virtus 3.5 L XL (The Virtis Co., Gardiner, NY) in a two-stage process. In the first stage, the HPLC solvent buffer methanol was evaporated until dryness. The white powder obtained was rehydrated with 15 mL of nanopure water, frozen rapidly by immersion in liquid nitrogen, and freeze-dried to yield white powder samples. A small fraction of each isolate was resolublized in methanol and analyzed by LC-MS/UV.

For adduct **II**, the optimal conditions for sample purification were as follows: 30 mmol of glucose, 90 mmol of glycine, and 10 mmol of ferulic acid were reacted in 20 g of sand with 4 mL of water (yield was 4-fold higher in comparison to model B). The reaction mixture was extracted with 200 mL of methanol for 30 min, filtered, and evaporated until dryness, and the residue was dissolved in 10 mL of 10% methanol aqueous solution. The mixture was loaded over an activated C-18 Sep-Pak (50 g Resprep, Restek, Bellefonte, PA) maintaining a flow rate of 1 mL/min. The Sep-Pak was washed with 25 mL of nanopure water followed by elution with 6 mL of methanol. The methanol extract was concentrated until precipitate appeared and filtered using a PTFE tip filter (0.45 μm). The filtered methanol extract was further fractionated using the same instrument as previously described for analyte **I** with minor modification. The elution gradient for the binary solvent system consisted of a series of linear gradients of B in A starting at 20% B in A (0−20 min), increasing to 90% B in A (20−22 min), and then held at 90% for 3 min (22−25 min), decreasing to 10% B in A (25−26 min), and held at 10% for 6 min (26−34 min). Two peaks with an m/z 383 $[M-1]^-$, which were 2.2 min apart in retention time (see **Figure 7**), were collected over approximately 90 independent injections, subsequently pooled, frozen at −20 °C, and then freeze-dried in the same two-stage process as for adduct **I**.

For analyte **IIa**, the optimal reaction conditions for sample purification were as follows: 12 mmol of glucose and 40 mmol of glycine were reacted with 15 g of sand with 2 mL of water. The filtered methanol extract was further fractionated using the same instrument as previously described for analyte **I** with minor modifications. The elution gradient for the binary solvent system consisted of a series of linear gradients of B in A starting at 20% B in A (0−10 min), increasing to 50% B in A (3−20 min), increasing to 90%B in A (20−23 min), and then held at 90% for 3 min (23−26 min), decreasing to 10% B in A (26−27 min), and held at 10% for 6 min (27−33 min) prior to the next injection. Analyte **IIa** was collected over approximately 90 independent injections, subsequently pooled, frozen at −20 °C, and then freeze-dried in Freezemobile 12 (The Virtis Co.) in the same two-stage process as for adduct **I**.

The isolates (ca. 5−10 mg) were dissolved in 0.6 mL of DMSO for adduct **I** and CD_3OD for adducts **II** and **IIa**. The sample spectra were recorded on a Bruker DRX-400 instrument (Bruker Biospin Co., Billerica, MA), and the chemical shifts (δ values) were referenced to the ^1H or ^{13}C chemical shifts of the internal standard trimethylsilane. ^1H, ^{13}C, gradient selected $^1H-^1H$ correlation spectroscopy (COSY), gradient-selected heteronuclear multiple quantum coherence (HMQC), and gradient-selected heteronuclear multiple bond coherence (HMBC) spectra were recorded at 400 MHz for ^1H and at 100 MHz for ^{13}C. $^1H-^1H$ COSY, HMBC, and HMQC two-dimensional (2D) NMR techniques were used to assign correlations between ^1H and ^{13}C signals.

Analysis of iNOS and COX-2 Expression by Western Blot Assays. RAW 264.7 macrophage-like cells, cultured in Dulbecco's Modified Minimum Essential Medium containing 5% fetal bovine serum, penicillin (100 IU/mL)−streptomycin (100 μg/mL), and 2 mM L-glutamine (all from Invitrogen, MD). The cells were treated with 25 μM each of adduct **I**, adduct **II**, and ferulic acid, or vehicle (DMSO) for 30 min followed by bacterial endotoxin LPS (1 μg/mL) for 12 h. These compounds had no effect on the viability of cells (data not shown). The cells were washed with ice-cold sterile phosphate-buffered saline and harvested by centrifugation at 2000*g*. The cell pellets were lysed using the mammalian protein extraction (M-PER) reagent containing protease inhibitor cocktail from Thermo Pierce (Rockford, IL). Total protein concentrations in each sample were estimated using the BCA reagent assay (Thermo Pierce). Equal amounts of protein from each sample were analyzed for the expression of iNOS and COX-2. Briefly, cell lysates were run on an SDS-PAGE gel (% T = 12.5), and the resolved proteins were transferred onto a nitrocellulose membrane as described earlier from our laboratory (*14*). Ponceau-S staining of the membrane was used to confirm uniform transfer of proteins to the membrane. The membrane was probed with anti-INOS or anti-COX-2 polyclonal antibodies (Cayman Chemicals, Ann Arbor, MI) or anti-GAPDH monoclonal antibody (Fitzgerald Industries, Concord, MA) as a housekeeping control. Appropriate horseradish peroxidase-conjugated anti-IgG antibody (Thermo Pierce) was used as the secondary antibody. The bands were visualized by using an enhanced chemiluminescence (ECL) assay kit (Thermo Pierce) according to the manufacturer's instructions. Autoradiographs were densitometrically evaluated using the Image J program from the National Institutes of Health.

RESULTS AND DISCUSSION

On the basis of a similar analytical approach previously applied by our laboratory to investigate the reactivity of the flavan-3-ols as influenced by Maillard chemistry in model and food systems (*15*−*20*), labeling studies were applied in the current study to investigate the reactivity of hydroxycinnamic acids in simple glucose/glycine model systems. Reaction products generated between the hydroxycinnamic acids and Maillard-type precursors or intermediates were analyzed within the detection limits of the LC-MS (< 2000 Da). Identified reaction products, those that consisted of a phenolic and glucose and/or glycine moiety, were isolated and structurally elucidated; on the basis of retrosynthesis, reaction pathways were suggested and further supported. Defined mechanisms of phenolic reactivity on Maillard chemistry were further correlated to the generation of

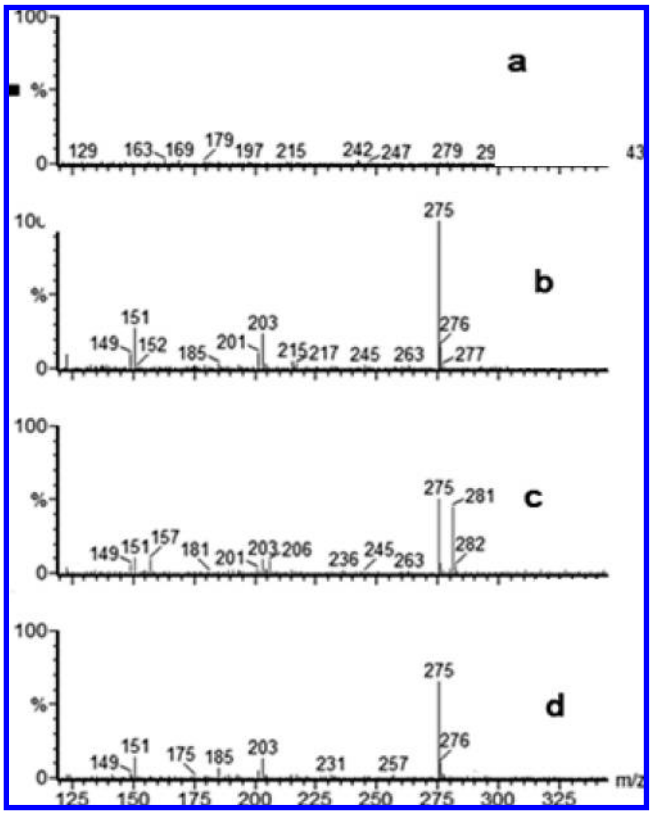

Figure 1. Mass spectrum of analyte MW 276 (*m/z* 275 [M − 1]$^-$) at retention time of 18.52 min generated from models: (**a**) glucose + glycine; (**b**) glucose + glycine + ferulic acid; (**c**) glucose($^{13}C_6$:$^{12}C_6$, 1:1) + glycine + ferulic acid; (**d**) glucose + glycine([$^{13}C_2$,^{15}N]:[$^{12}C_2$, ^{14}N], 1:1) + ferulic acid.

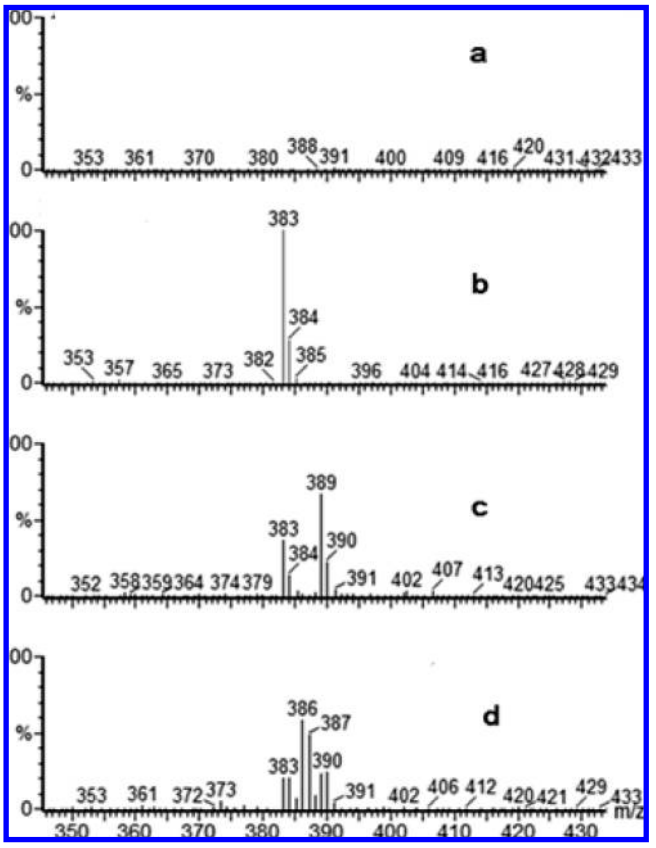

Figure 2. Mass spectrum of analyte MW 384 (*m/z* 383 [M − 1]$^-$) at retention time of 19.89 min generated from models: (**a**) glucose + glycine; (**b**) glucose + glycine + ferulic acid; (**c**) glucose($^{13}C_6$:$^{12}C_6$, 1:1) + glycine + ferulic acid; (**d**) glucose + glycine ([$^{13}C_2$,^{15}N]:[$^{12}C_2$, ^{14}N], 1:1) + ferulic acid.

Maillard-type volatile compounds and color development in these model systems as well as to the anti-inflammatory bioactivity of these phenolic reaction products.

Identification of Hydroxycinnamic Acid−Maillard Adducts: Isotopomeric Analysis. LC-MS isotopomeric analysis of simple glucose/glycine model systems consisting of a 1:1 ratio of unlabeled to labeled glucose (*21*) and a 1:1 ratio of unlabeled to labeled glycine (*22*) with ferulic acid as well as unlabeled glucose/glycine with and without a hydroxycinnamic acid (**Table 1**, models A−D) were used to identify hydroxycinnamic acid−Maillard reaction products. Analytes selected by LC-MS analyses consisted of (i) isotopomers reported in models C and/or D, and (ii) the parent ion for these analytes was also detected in model B but not detected in model A, at the same peak retention time. Two main ferulic acid−Maillard adducts were detected in the model systems with the predicted molecular weights of 276 and 384 (based on pseudomolecular ion [M − 1]$^-$). The mass spectrum for these model systems for MW of 276 termed adduct **I** is displayed in **Figure 1**, whereas that for the MW 384 compound termed adduct **II** is displayed in **Figure 2**. The [M − 1]$^-$ + 6 isotopomer detected in **Figure 1**, model C, indicated that adduct **I** consisted of an intact C6 sugar fragment. The composition of adduct **I** was also confirmed not to contain any glycine component as the analogous 1:1 glycine unlabeled to labeled models (model D) did not report any detectable isotopomers in these model systems. Adduct **II** also had an [M − 1]$^-$ + 6 isotopomer (**Figure 2**) for model C or consisted of an intact C6 sugar fragment, whereas for model D (**Figure 2**) 5 isotopomers plus M were observed, consisting of M + 1, M + 3, M + 4, M + 6, and M + 7 with a 1:1:2:2:1:1 abundance, which indicated it consisted of two intact glycine moieties and another carbon or nitrogen atom from glycine. In an analogous reaction to **Figure 2d**, but without labeling the N (model G), the signal atom from glycine was concluded to be carbon.

These results were consistent with reactivity of the flavan-3-ols in similar model systems where the main phenolic−Maillard adduct reaction products consisted of C5 and C6 sugar fragment products under low-moisture conditions (*20*), whereas under aqueous conditions the main reaction products consisted of C2, C3, and C4 sugar fragments (*18*). Peterson and Noda (*5*) likewise reported that in aqueous models ferulic acid also generated phenolic−C2, −C3, and −C4 sugar fragment reaction products. However, in both aqueous and low-moisture models the flavan-3-ols were not reported to react with glycine, whereas the hydroxycinnamic acids were reported to react with glycine to generate phenolic−Maillard reaction product adducts (*16*). In alkalized cocoa, glycosylated flavan-3-ols have been reported (*23*).

Structural Elucidation of Adducts I and II: MS-TOF and NMR Analysis. *Adduct I.* In addition to the compositional information from the isotopomeric analysis for adduct **I**, phenolic plus an intact C6 sugar moiety, MS-Tof analysis reported a molecular weight of 275.0919 (M − 1)$^{-1}$ with the predicted formula for pseudomolecular ion of $C_{15}H_{16}O_5$ (0 ppm). NMR analysis also indicated 12 and 15 resonance signals were detected in the ^{1}H and the ^{13}C NMR spectra (**Tables 2** and **3**), further supporting the molecular formula of $C_{15}H_{16}O_5$. On the basis of these findings as well as 2-D NMR analysis (HMBC, **Table 3**; COSY, **Table 2**), the molecular structure of adduct **I** was determined to be 6-(4-hydroxy-3-methoxyphenyl)-5-(hydroxymethyl)-8-oxabicyclo[3.2.1]oct-3-en-2-one (shown in **Figure 3**). The chemical shifts and coupling constants of three aromatic protons, H−C(5),

H−C(3), and H−C(6), and another proton, H−C(7), from the methyl group, compared with the ^{1}H spectra of a decarboxylated ferulic acid (2-methoxy-4-vinylphenol, data not shown), indicated the transfer of the 2-methoxyphenol moiety from ferulic acid to adduct **I**. This is further strengthened by a HMBC cross peak between H−C(7) and another aromatic carbon C(2), which is also correlated with three aromatic protons in the HMBC spectrum. HMBC correlation of H−C(5), H−C(3), and H−C(6) to C(8) indicated that the 4-position of the benzene ring was substituted by C(8). COSY correlation of H−C(8)/H_a−C(9), H_b−C(9)/H−C(1′), combined with their coupling constants in the ^{1}H spectra, suggested the connection of C(8)−C(9)−C(1′). HMBC correlation of H−C(1′) and one olefinic H−C(3′) to the same carbonyl carbon C(2′) permitted the connection of C(1′)−C(2′)−C(3′)−C(4′). HMBC also showed that H−C(8), H−C(6′), and H−C(4′) were correlated to the same quaternary carbon C(5′) and, in conjunction with the fact that there were no vicinal couplings between these three protons, confirmed the proposed linkage between these four relevant carbons in **Figure 3**. H−C(1′) and H−C(6′) resonating at relative low field respectively indicated C(1′) and C(6′) were connected to the heteroatom, oxygen in this case. In addition, HMBC correlation between H−C(1′) and C(5′), combined with chemical formula and degree of unsaturation, unambiguously revealed the proposed structure in **Figure 3**. Interestingly, adduct **I** and other structurally similar compounds have been previously reported in plant extracts used in traditional Chinese medicine (*24*, *25*). The NMR data for the compounds identified in the plant extracts were also in agreement with this study and were furthermore used to assign the endo stereochemistry of adduct **I** by characteristic vicinal coupling between H−C(8) and H_a (7.2 Hz) and between H−C(8) and H_b (10.2 Hz) according to spectral data for descurainin (*24*). The coupling constant between endo proton (H_a) and H−C(1′) was much less than the one between exo proton (H_b) and H−C(1′) according to their dihedral angles. The minor isomer was assigned as the exo isomer accordingly because these two coupling constants were changed to 8.9 and 3.4 Hz, respectively. The ratio of endo to exo was determined to be 4.5:1 according to integration result from the ^{1}H spectrum of the two-isomer mixture.

For adduct **II** MS-Tof analysis reported a molecular weight of 385.1407 $(M + 1)^{+1}$ with the predicted formula for pseudomolecular ion of $C_{20}H_{20}N_2O_6$ (1.8 ppm). The NMR spectra are summarized in **Tables 4** and **5**. On the basis of these techniques and the isotopomeric data, the structure of adduct **II** was reported to be 2-(6-(furan-2-yl)-7-(4-hydroxy-3-methoxyphenyl)-1-methyl-3-oxo-2,5-diazabicyclo[2.2.2]oct-5-en-2-yl)acetic acid (shown in **Figure 4**). In brief, a 2-substitued furan ring was deduced from the characteristic coupling pattern of the hydrogens H−C(6′)/H−C(5′)/H−C(4′) and was further confirmed by a double-quantum filtered homonuclear δ,δ correlation (DQF-COSY) experiment (**Table 4**). The chemical shifts of carbons C(1) and C(1″) and two carbonyl carbons C(2′) and C(2″), combined with strong HMBC correlation of H−C(1″) to carbonyl carbon C(2″) and a imine nitrogen (315 ppm), permit deduction of the reduced pyrazinone ring. No HMBC cross peak between H−C(3″) and any carbons in furan ring and also no HMBC correlation between any hydrogens in furan ring and C(3″),

Table 2. Assignment of ^{1}H NMR Signals (400 MHz, DMSO-d_6) for Adduct **I**

H at relevant C atom	δ	no. of H	type	J_{HH} (Hz)	COSY
H_a−C(9)	1.99	1	ddd	13.2	H_b−C(9)
				7.1	H−C(8)
				1.3	H−C(1′)
H_b−C(9)	2.91	1	ddd	13.2	H_a−C(9)
				10.3	H−C(8)
				8.9	H−C(1′)
H−C(8)	3.58	1	dd	10.3	H_a−C(9)
				7.1	H_b−C(9)
H_c−C(6′)	3.71	1	d	12.4	H_d−C(6′)
H_d−C(6′)	3.81	1	d	12.4	H_c−C(6′)
H−C(7)	3.79	3	s		
H−C(1′)	4.55	1	dd	8.9	H_b−C(9)
				1.3	H_a−C(9)
H−C(3′)	6.21	1	d	9.8	H−C(4′)
H−C(4′)	6.74	1	d	9.8	H−C(3′)
H−C(5)	6.61	1	dd	7.9	H−C(6)
				1.7	H−C(3)
H−C(3)	6.71	1	d	1.7	H−C(5)
H−C(6)	6.77	1	d	7.9	H−C(5)

Table 3. Assignment of ^{13}C NMR Signals (400 MHz, DMSO-d_6) for Adduct **I**

C atom	δ	type	HMBC
C(9)	34.8	CH_2	H−C(8), H−C(1′)
C(8)	48.2	CH	H_a−C(9), H_b−C(9), H−C(6′), H−C(1′), H−C(3), H−C(5)
C(7)	56.5	CH_3	
C(6′)	64.9	CH_2	H−C(8), H−C(4′)
C(1′)	81.9	CH	H_a−C(9), H−C(8), H−C(3′), H_b−C(9),
C(5′)	87.2	C	H−C(4′), H−C(8), H−C(1′), H−C(6′)
C(6)	113.7	CH	H−C(5)
C(3)	116.2	CH	H−C(5), H−C(8)
C(5)	122.4	CH	H−C(8), H−C(3), H−C(6)
C(3′)	128.9	CH	H_a−C(9), H_b−C(9), H−C(1′), H−C(4′)
C(4)	129.7	C	H−C(8), H−C(3), H−C(5), H−C(6)
C(1)	147.1	C	H−C(6)
C(2)	148.5	C	H−C(7), H−C(3), H−C(6)
C(4′)	155.4	CH	H−C(8), H−C(6′), H−C(3′)
C(2′)	199.2	C	H−C(1′), H−C(3′), H_a−C(9), H_b−C(9)

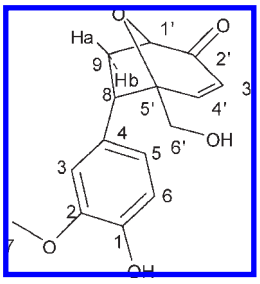

Figure 3. Molecular structure for adduct **I**, 6-(4-hydroxy-3-methoxyphenyl)-5-(hydroxymethyl)-8-oxabicyclo[3.2.1]oct-3-en-2-one). Carbon atoms labeled 1−9 originate from ferulic acid moiety, and those labeled 1′−6′ originate from glucose moiety.

Table 4. Assignment of ^{1}H NMR Signals (400 MHz, DMSO-d_6) of Adduct **II**

ID	[H]	no. of H	type	J_{HH} (Hz)	COSY
H−C(5″)	1.66	3	s		
H_a−C(9)	1.88	1	ddd	13.2, 5.6	H_b−C(9), H−C(8)
				3.4	H−C(1″)
H_b−C(9)	2.64	1	dd	13.2, 10.1	H_a−C(9), H−C(8)
H−C(7)	3.54	3	s		
H−C(8)	3.57	1	dd	5.6, 10.1	H_b−C(9), H_a−C(9)
H_c−C(3″)	4.04	1	d	17.1	H_d−(3″)
H_d−C(3″)	4.14	1	d	17.1	H_c−(3″)
H−C(1″)	4.94	1	d	3.4	H_a−C(9)
H−C(3)	6.44	1	s		
H−C(5′)	6.50	1	dd	3.5, 1.6	H−C(4′), H−C(6′)
H−C(5)	6.54	1	d	8.2	H−C(6)
H−C(6)	6.59	1	d	8.2	H−C(5)
H−C(4′)	6.89	1	d	3.5	H−C(5′)
H−C(6′)	7.64	1	d	1.6	H−C(5′)

Table 5. Assignment of ^{13}C NMR Signals (400 MHz, DMSO-d_6) of Adduct **II**

C atom	δ	type	HMBC
C(5″)	18.2	CH_3	H−C(8)
C(9)	33.2	CH_2	H−C(8)
C(3″)	45.3	CH_2	
C(8)	52.1	CH	H−C(3), H_a−C(9), H_b−C(9), H−C(5)
C(7)	57.2	CH_3	
C(1′)	63.4	C	H−C(3″), H−C(8), H−C(5″)
C(1″)	64.6	CH	H_a−C(9), H_b−C(9)
C(3)	112.4	CH	H−C(8), H−C(5)
C(5′)	113.0	CH	H−C(4′), H−C(6′)
C(6)	116.4	CH	H−C(5)
C(4′)	117.0	CH	H−C(5′), H−C(6′)
C(5)	124.2	CH	H−C(6), H−C(3), H−C(8),
C(4)	132.5	C	H−C(5), H−C(6), H−C(3)
C(6′)	146.1	CH	H−C(4′), H−C(5′)
C(1)	146.9	C	H−C(6)
C(2)	149.1	C	H−C(7), H−C(3)
C(3′)	151.1	C	H−C(4′), H−C(5′), H−C(6′)
C(2′)	165.7	C	
C(2″)	167.8	C	H−C(1″)
C(4″)	175.3	C	H−C(3″)

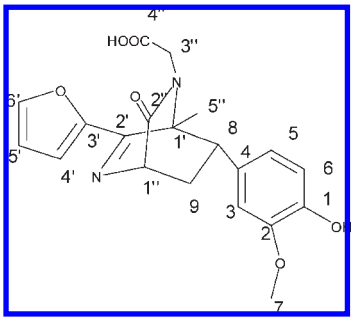

Figure 4. Molecular structure for adduct **II**, 2-(6-(furan-2-yl)-7-(4-hydroxy-3-methoxyphenyl)-1-methyl-3-oxo-2,5-diazabicyclo[2.2.2]oct-5-en-2-yl)-acetic acid. Carbon atoms labeled 1−9 originate from ferulic acid moiety, those labeled 1′−6′ originate from glucose moiety, and those labeled 1″−5″ originate from glycine moiety.

combined with the obvious fact that the furan moiety comes from one and only one glucose moiety in this compound, can assign C(3″) to be C-2 of one intact glycine moiety. HMBC correlations of H−C(3″) to carboxylic acid carbons C(4″), C(1′), and C(2″) allowed the connection of this intact glycine moiety to the pyrazinone ring. Similar to adduct **I**, the NMR spectra for adduct **II** also reported the 2-methoxyphenol moiety of ferulic acid. COSY correlation between H−C(9) and H−C(1″), combined with HMBC correlation between H−C(8) and C(1′), established the connection between the phenolic moiety and the pyrazinone ring. Methyl group C(5″) was assigned to be connected to aliphatic carbon C(1′) rather than to the polarized imine carbon C(2′) because its ^{13}C signal is resonating at very high field. Another correlation between methyl group H−C(5″) and the other nitrogen atom resonating at 150 ppm also confirmed the connectivity between C (5″) and C (1′). The proposed structure was also confirmed by its direct intermediate **IIa** structure identification in the following section.

Mechanisms of Adduct I and II Generation. A reaction mechanism for adduct **I** 6-(4-hydroxy-3-methoxyphenyl)-5-(hydroxymethyl)-8-oxabicyclo[3.2.1]oct-3-en-2-one) is illustrated in **Scheme 1**. Ferulic acid was suggested to undergo decarboxylation, facilitated by the *p*-phenol hydroxyl group (*26*), to generate 2-methoxy-4-vinylphenol. In a parallel reaction, 3-deoxy-2-hexosulose generated by Amadori degradation was further

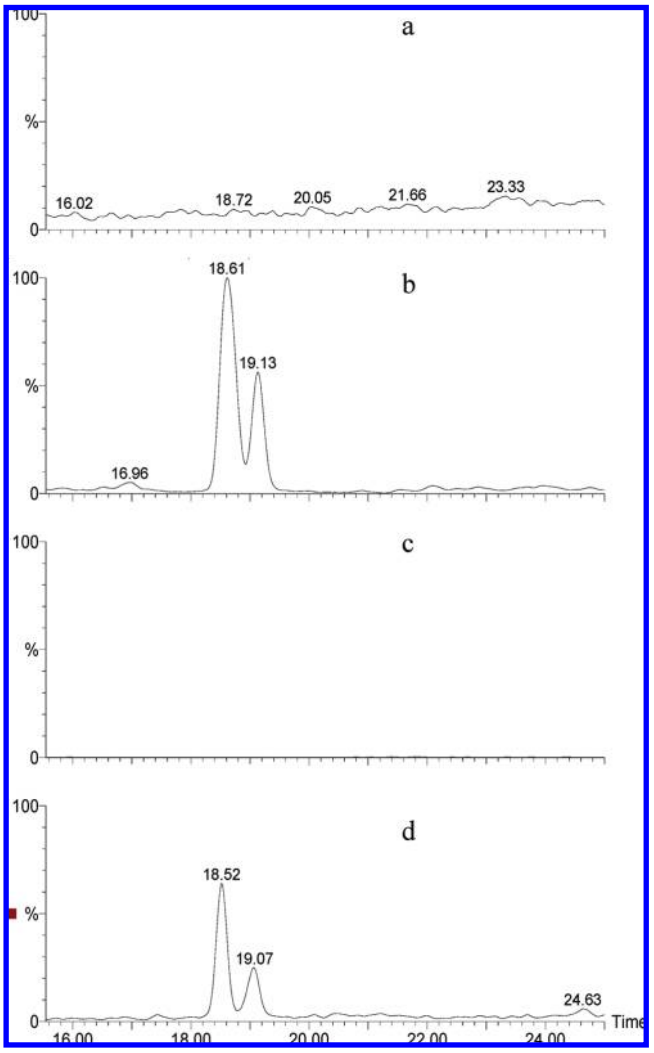

Figure 5. LC-MS chromtogram of analyte MW 276 (*m*/*z* 275 [M − 1]$^-$) generated from models: (**a**) glucose + glycine; (**b**) glucose + glycine + ferulic acid; (**c**) glucose + ferulic acid; (**d**) 3-dexoxy-2-hexosulose+ 2-methoxy-4-vinylphenol. The peak at 18.5 min is an endo product, and the peak at 19.1 min is an exo product.

dehydrated/cyclized to generate an oxopyrylium zwitterion, which reacted with 2-methoxy-4-vinylphenol by 5,2-cycloaddition to produce adduct **I**. A chromatogram of adduct **I** generated in a glucose/glycine/ferulic acid model is illustrated in **Figure 6b**; no similar products were observed for glucose and glycine (**Figure 6a**). The two peaks illustrated in **Figure 6b** are the exo and endo isomers reported in **Scheme 1**. Although caramelization of glucose would be expected to occur in these model reactions (200 °C), which could generate sugar degradation products such as 3-deoxy-2-hexosulose, a reaction between glucose and ferulic acid (**Figure 5c**) did not generate the phenolic−C_6 sugar adduct, signifying glycine was important for the generation of this phenolic reaction product and likely that 3-deoxy-2-hexosulose was generated by Maillard pathways. To further support the reaction mechanism in **Scheme 1**, 2-methoxy-4-vinylphenol and 3-deoxy-2-hexosulose were directly reacted and did generate adduct **I** (see **Figure 6d**).

Further analysis of other common dietary hydroxycinnamic acids (*p*-coumeric, sinapic, and caffeic acid) in model B (glucose/glycine + phenolic) as anticipated generated analogous adduct **I** reaction products (shown in **Figure 6a**−**c**). The identities of these reaction products were supported by accurate mass TOF analysis;

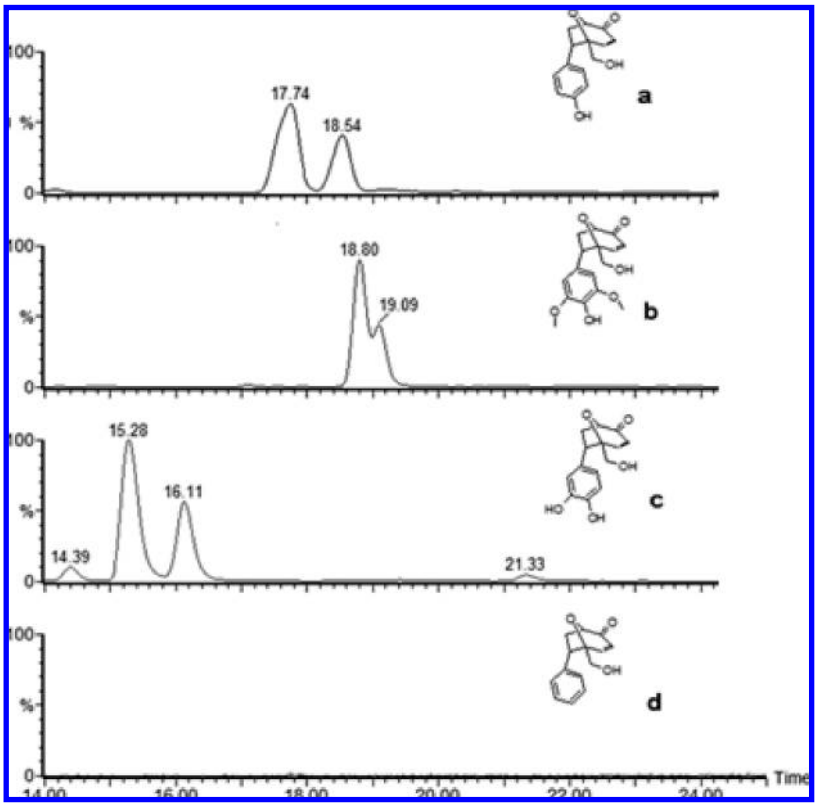

Figure 6. Chromatogram of analogous compounds of adduct **I** generated by (**a**) *p*-coumaric, (**b**) sinapic, (**c**) caffeic, or (**d**) cinnamic acid in glucose/glycine model reactions.

Scheme 1. Mechanism for Adduct **I** Generation

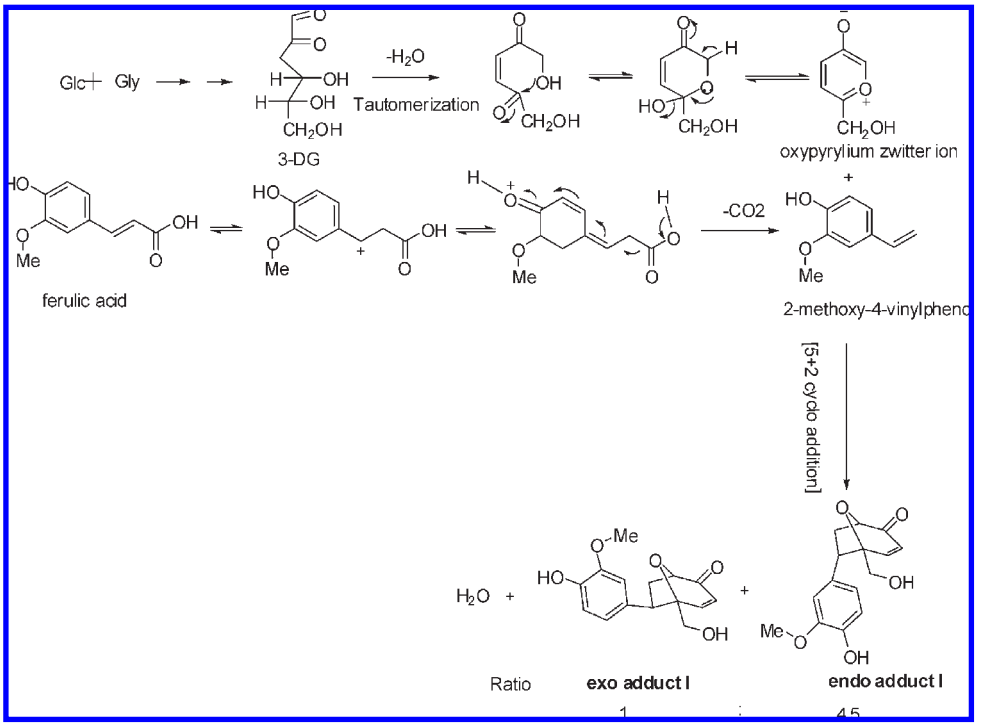

all compounds were within 5 ppm error (data not shown). Cinnamic acid was also analyzed but because it does not have a *p*-phenol hydroxyl group, it did not undergo decarboxylation and, therefore, cannot form a more reactive dipolarophile; therefore, the corresponding decarboxylated adduct was not detected (**Figure 6d**). However, a trace amount of the non-decarboxylated product analogous adduct **I** was observed. The three phenolic−Maillard reaction products reported in **Figures 3** and **5a**,**b** have been previously identified as natural products in various Chinese medicinal plants (*24*, *25*, *27*).

The mechanism of generation for adduct **II** 2-(6-(furan-2-yl)-7-(4-hydroxy-3-methoxyphenyl)-1-methyl-3-oxo-2,5-diazabicyclo[2.2.2]oct-5-en-2-yl)acetic acid is illustrated in **Scheme 2**. The chromatogram for adduct **II** is shown in **Figure 7**; the two peaks

represent the endo and exo isomers (**Scheme 2**). Similar to adduct **I**, ferulic acid was decarboxylated to 2-methoxy-4-vinylphenol, which underwent a 4 + 2 cycloaddition reaction with a 2-(furan-3-yl)-3-methylpyrazinone to generate adduct **II**. Alkyl-substituted pyrazinone compounds are known to be formed by multiple glycine addition to glucose in glycine/glucose model systems. A series of 2-(3′-alkyl-2′-oxopyrazin-1′-yl)alkyl acids or pyrazinones, which were characterized by various spectroscopic techniques, were identified by Chuyen et al. (*28*) in a dipeptides/glucose system. Yaylayan et al. (*29*) also reported the decarboxylated analogues of these pyrazinones in a glucose/glycine model system.

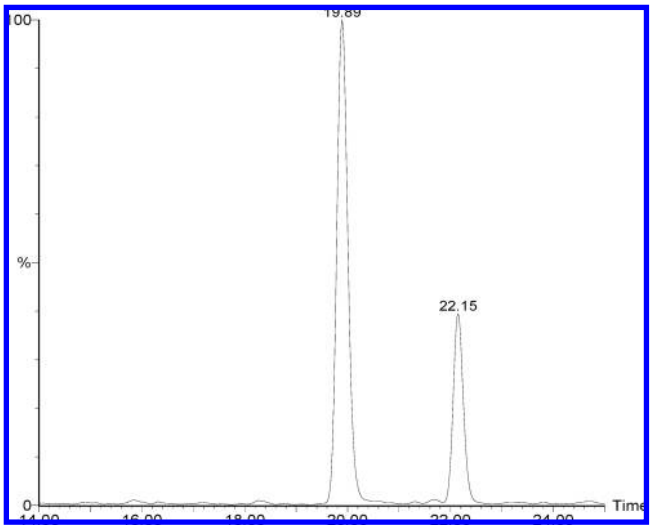

Figure 7. Chromtogram of adduct **II** generated from glucose/glycine/ferulic acid reaction. The peak at 19.91 min is an endo product, and the peak at 22.13 min is an exo product.

The mechanisms of pyrazinone generation and C-2 glycine methylation were also previously described by Yaylayan using a pyrolysis glucose/glycine system (*29*). In our model system, the pyrazinone (**IIa**) was suggested to be formed by direct glycine addition to an Amadori product. It was anticipated the pyrazinone ring formation was aided by the aldol condensation reaction with formaldehyde, a Strecker aldehyde of glycine. The resulting double bond was directly attached to the ring and, thus, can easily shift to form an endocyclic double bond to release ring strain. Because diene-containing compounds with heteroatoms normally go through Diels−Alder reactions with inverse electron demand, adduct **II** should be formed by cycloaddition reaction between precursor **IIa** and electron-rich dienophile 2-methoxy-4-vinylphenol rather than ferulic acid. Regioselectivity of adduct **II** was determined by NMR analysis, whereas its stereoselectivity was determined according to the endo rule of the Diels−Alder reaction.

To further confirm **Scheme 2**, the pyrazinone (**IIa**, **Figure 8**) was isolated from model A (glucose/glycine) and the molecular structure was confirmed by MS-Tof accurate mass (235.0725, 2.6 ppm) and NMR techniques (**Table 6**; **Figure 8**). A direct reaction between the pyrazinone (**IIa**) and 2-methoxy-4-vinyl-

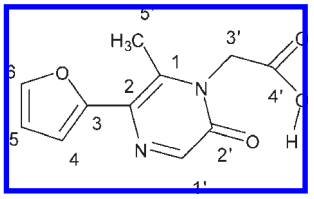

Figure 8. Proposed structure of pyrazinone-type precursor **IIa** for adduct **II**. Carbons labeled 1−6 originate from glucose moiety, and those labeled 1′−6′ originate from glycine moiety.

Scheme 2. Mechanism for Adduct **II** Generation

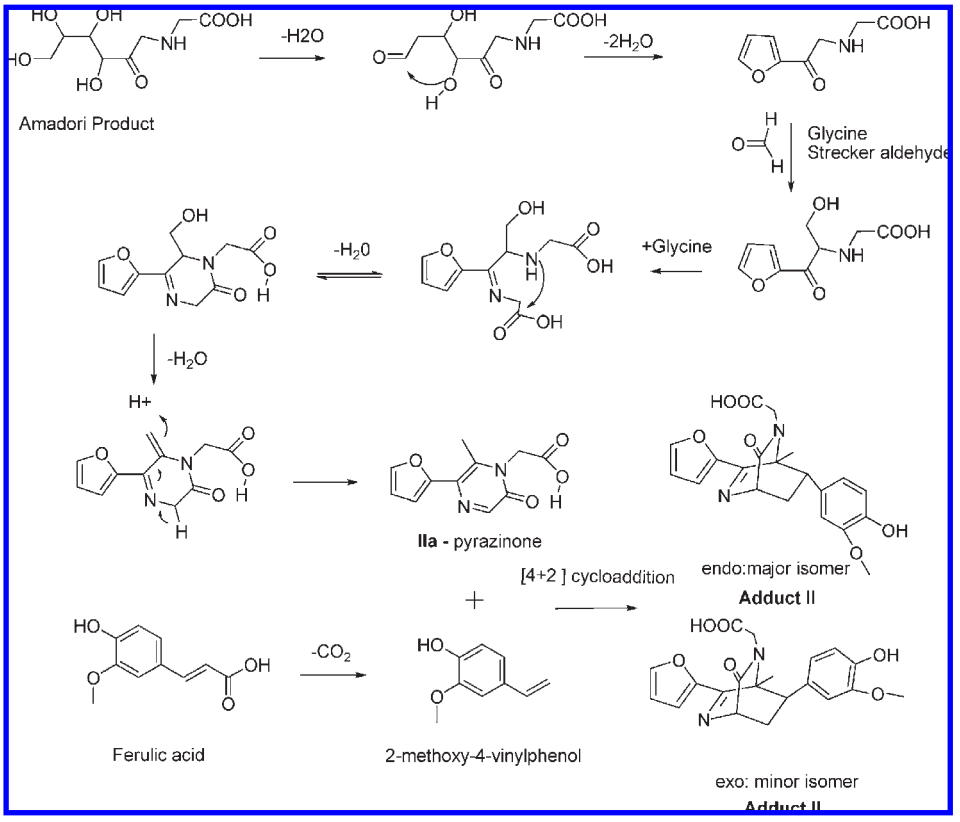

Table 6. Assignment of ^{1}H and ^{13}C NMR Signals (400 MHz, DMSO-d_6) of Intermediate **IIa**

C atom	δ	type	H at relevant C atom (ppm)	J_{HH} (Hz)	COSY	HMBC
C(5′)	16.1	CH_3	2.51 (s)			
C(3′)	46.3	CH_2	4.5 (s)			
C(4)	113.2	CH	6.67 (d)	3.2	H-C(5)	H−C(5)
						H−C(6)
C(5)	119.3	CH	6.61 (dd)	1.6	H−C(4)	H−C(4)
				3.2	H−C(6)	H−C(6)
C(2)	125.3	C				H−C(5′), H−C(1′)
C(1)	139.5	C				H−C(5′), H−C(3′), H−C(1′)
C(6)	150.1	CH	7.71 (d)	1.6	H−C(5)	H−C(4), H−C(5)
C(1′)	152.1	CH	8.01 (s)			H−C(5′)
C(3)	162.2	C				H−C(5′), H−C(4) H−C(5), H−C(6)
C(2′)	168.2	C				H−C(1′), H−C(3′)
C(4′)	180.1	C				H−C(3′)

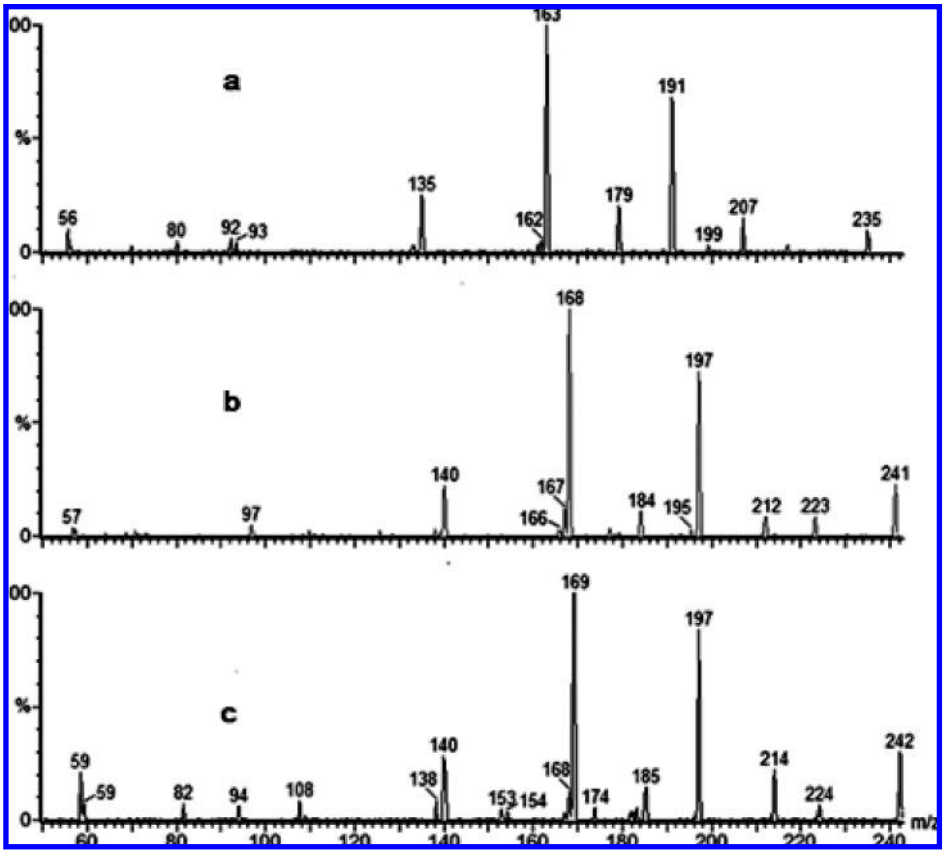

Figure 9. MS sibling ion spectra of (**a**) *m*/*z* 235, (**b**) isotopomeric ion at *m*/*z* 241 from glucose ($^{13}C_6$:$^{12}C_6$, 1:1) + glycine + ferulic acid, and (**c**) *m*/*z* 242 glucose + glycine([$^{13}C_2$,^{15}N]:[$^{12}C_2$, ^{14}N], 1:1) + ferulic acid.

phenol generated adduct **II** (**Figure 4**) and did regenerate the chromatogram illustrated in **Figure 7** (data not shown).

One of the main fragmentation ions observed by LC-MS analysis of adduct **II** was the precursor pyrazinone (**IIa**), which was easily generated by "in-source" collision (data not shown). On the basis of "in-source" collision of adduct **II** and subsequent sibling ion analysis of this pyrazinone compound (MS^3, sibling ions ← 235 ← 385), the ion fragmentation spectrum is illustrated in **Figure 9a** and the related MS fragmentation scheme is presented in **Scheme 3**. Further fragmentation analysis of the M + 6 isotopomer form model C (fully labeled glucose moiety) and the M + 7 isotopomer form model D (2 fully labeled glycine + 1 labeled carbon from glycine) was conducted and illustrated in **Figures 9**, panels **b** and **c**, respectively. Review of the unlabeled and labeled fragmentation patterns further supported the molecular structure of adduct **II** (**Figure 4**) and intermediate **IIa**. For example, the iminium fragment of *m*/*z* of 56 (**Scheme 3**; **Figure 9a**) generated a corresponding *m*/*z* of 57 for the fully labeled glucose moiety (**Figure 9b**) and an *m*/*z* of 59 for the fully labeled glycine moiety (**Figure 9c**) as predicted on the basis of the incorporation of one carbon-13 atom from glucose (C1′, **Figure 4**) and two carbon-13 (C3″ and C5″, **Figure 4**) and one nitrogen-15 atoms from glycine. Similar results were reported for the remaining observed ion fragments.

Quantitative Analysis of Reactants/Products in Models. To gain further insight into the reactivity of hydroxycinnamic acids in Maillard-type chemistry model systems, quantitative analysis was conducted to monitor the stability of ferulic acid, the generation of the decarboxylated ferulic acid intermediate (2-methyl-4-vinylphenol), and the generation of adducts **I** and **II** (**Table 7**) as well as the influence of ferulic acid on the generation of Maillard-type aroma compounds (**Table 8**) and color development.

Scheme 3. Tandem MS-ESI Positive Sibling Ion Fragmentation for Adduct **II**

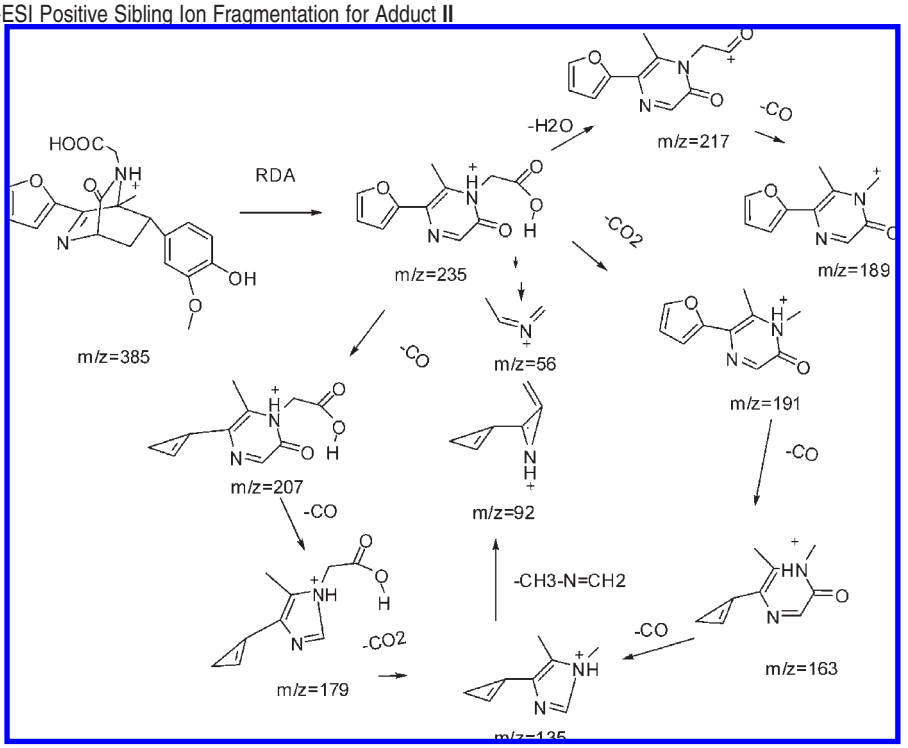

Table 7. Stability of Ferulic Acid and Quantities of 2-Methoxy-4-vinylphenol and Adducts **I** and **II** Generated in Models B and I[a]

		% yield (based on ferulic acid)		
model	% residual ferulic acid	2-methoxy-4-vinylphenol	adduct **I**	adduct **II**
B	4.6	31.2	0.3	0.1
I	83.5	8		

[a] Model B was 3 mmol of ferulic acid, glucose, and glycine; model I was 3 mmol of ferulic acid; in 15 g of quartz sand and 1.5 g of water, heated at 200 °C for 15 min.

The stability of ferulic acid when reacted with equimolar amounts of glucose/glycine (model B) was reduced in comparison to when ferulic acid was reacted by itself (model I), reporting 4.6 and 83.5% residual levels after each reaction, respectively (**Table 7**). In agreement with the stability analysis of ferulic acid, a 5-fold higher amount of 2-methoxyl-4-vinylphenol (degradation product of ferulic acid) was reported in model B versus model I. The yields of adducts **I** and **II** generated were 3 and 1%, respectively (**Table 7**). The mass of the two adducts and 2-methyl-4-vinylphenol accounted for < 50% of the ferulic acid degraded. Styrene-type structures, such as 2-methoxy-4-vinylphenol, are well-known to undergo oligomerization (*30*) and likely contribute to the undefined ferulic acid degradation products in model B. An increase in the carbohydrate reactant ratio was also reported to increase the formation of adduct **I**, whereas an increase in the amino acid reactant ratio resulted in an increased generation of adduct **II** (data not shown).

Ferulic acid was also reported to influence the generation of aroma compounds in these model reactions. The most abundant volatile compounds based on GC peak area detected in the glucose/glycine model system (model A) were identified, quantified, and compared to model B (with ferulic acid) and model H (with 2-methyl-4-vinylphenol) (see **Table 8**). Overall, the addition of ferulic acid significantly reduced the quantity of heterocyclic nitrogen-containing aroma compounds such as 2,5-dimethylpyrazine, 2,3,5-trimethylpyrazine, and 2-acetylpyridine, as well as the oxygen-containing heterocyclic compounds cyclotene and 2-acetylpyrrole, whereas the quantities of furfural and 5-methylfurfural were increased with no significant change in the generation for 2-acetylfuran. The low-moisture model systems used in this study would not consist of a solution; however, the addition of an acidic moiety (ferulic acid) could potentially alter the mechanisms of the Maillard reaction and product development. Because the decarboxylated ferulic acid was suggested to be a reactive phenolic precursor for the reaction mechanisms proposed in **Schemes 1** and **2**, and was not an acid, an additional glucose/glycine reaction with this precursor was analyzed (model H). A third amount of 2-methyl-4-vinylphenol was added in comparison to ferulic acid based on the amount quantified in model B (**Table 7**). In general, a similar pattern of Maillard-type product modification was observed for the decarboxylated ferulic acid in comparison to ferulic acid (**Table 8**). This suggested acid catalysis was not the only mechanism by which ferulic acid modified Maillard chemistry.

Color development in a glucose/glycine model was also influenced by ferulic acid addition. The absorbance measured at 420 nm for an aqueous extract was 4-fold higher in model A (glucose/glycine) than in model B (glucose/glycine/ferulic acid) at 0.12 and 0.44, respectively. Consequently ferulic acid addition altered the browning reaction in these Maillard models. Pyrazinone-type intermediates, such as **IIa**, have been reported to accelerate browning reactions (*28*), and thus ferulic acid could have had an inhibitory effect by scavenging this browning precursor as suggested in **Scheme 2**. Sulfite, in addition to reacting with carbonyl groups, has also been suggested to suppress the Maillard reaction by trapping melanoidin precursors by generating sulfite−melanoidin precursor adducts (*31*). In addition, ferulic acid has been recently reported to be incorporated into coffee brew melanoidins with a C−C bond, but the mechanism remains obscure (*32*). Cycloaddition mechanisms reported in this study could provide a mechanism for ferulic acid incorporation in coffee melanoidins.

On the basis of the reported reactivity of ferulic acid in our Maillard models (**Schemes 1** and **2**) it was still not known how hydroxycinnamic acids altered Maillard-type aroma generation. These findings do, however, suggest that the phenolic component of whole grain foods can alter Maillard-type flavor development

Table 8. Concentration of Select GC Analytes in Models A, B, and H

	concn[a] (μmol/mmol of glucose)			ratio	
	model A	model B	model H	model B/model A	model H/model A
furfural	0.301 ± 0.077	0.612 ± 0.058	0.371 ± 0.067	2.02	1.23
2-acetylfuran	0.087 ± 0.014	0.077 ± 0.008	0.068 ± 0.013	0.88	0.77
2,5-dimethylpyrazine	0.012 ± 0.003	0.003 ± 0.000	0.008 ± 0.000	0.26	0.57
5-methylfurfural	0.342 ± 0.052	0.489 ± 0.059	0.305 ± 0.030	1.43	0.89
2,3,5-trimethylpyrazine	0.005 ± 0.000	0.001 ± 0.000	0.004 ± 0.000	0.16	0.73
cyclotene	0.119 ± 0.037	0.0112 ± 0.003	0.112 ± 0.011	0.09	0.94
2-acetylpyridine	0.018 ± 0.002	0.011 ± 0.001	0.012 ± 0.001	0.60	0.66
2-acetypyrrole	0.021 ± 0.003	0.009 ± 0.005	0.0169 ± 0.002	0.45	0.81

[a] Mean of triplicate ± 95% confidence interval; model A was 3 mmol of glucose and glycine; model B was 3 mmol of ferulic acid, glucose, and glycine; model H was 1 mmol of 2-methoxy-4-vinylphenol plus 3 mmol of glucose and glycine.

in foods and may relate to the lower acceptability of whole grain foods such as bread (*2*). The scavenging of free radicals by hydroxycinnamic acids may also relate to Maillard chemistry changes observed in our models. Free radicals, such as enaminols and pyrazinium radical cations, are known to participate in Maillard browning (*6*, *33*−*37*).

Bioactivity of Ferulic Acid, Adduct I, and Adduct II. The health-promoting properties of whole grain foods have been linked to the hydroxycinnamic acid derivatives (*1*, *13*). Because these compounds are consumed as food products, it is possible the chemical modification of these native phenolic compounds during food processing, such as by the Maillard reaction as defined in this study, could relate to the epidemiological evidence supporting the positive health impact of consuming whole grain foods. To examine if food-modified phenolic compounds may be related to the health benefits of whole grain foods, the two phenolic−Maillard adducts along with ferulic acid were compared for their ability to suppress the expression of pro-inflammatory genes in macrophages stimulated with the bacterial endotoxin LPS. As shown in **Figure 10**, adducts **II** and **I** strongly suppressed the LPS-induced expression of both iNOS and COX-2 compared to ferulic acid. In fact, adduct **II** appeared to be more potent compared to adduct **I**. Both iNOS and COX-2 are key players in inflammation, which is pivotal for the development and progression of many chronic diseases. The reported bioactivity of adducts **I** and **II** to suppress iNOS and COX-2 suggests the reduction in chronic disease associated with whole grain consumption may be, in part, related to phenolic reaction products generated during food processing. Mechanistically, these adducts may have resulted in a higher strength antioxidant in comparison to ferulic acid; however, it is more likely these compounds altered the complex cellular signaling cascades up-regulating the expression of COX-2 and iNOS. To our knowledge, this is the first report that provides a molecular basis underlying the health benefits of these thermally generated adducts. Needless to say, the impact of these novel adducts on the upstream signal transduction pathways needs to be further characterized. Consequently, defining phenolic−Maillard reactions in foods may identify key biomarkers for the development of novel food-processing technology to tailor food products for improved health impact.

In summary, the addition of hydroxycinnamic acids to a simple glucose/glycine baking model was reported to alter the biochemistry of both the hydroxycinnamic acids and the mechanisms of the Maillard reaction and Maillard-type product generation. The phenolic−Maillard interactions identified provide a new food chemistry reaction mechanism to investigate the flavor development and health promotion of whole grain foods. The negative flavor properties of whole grain foods may be related to phenolic-induced changes in Maillard-type flavor development as reported in our models. Furthermore, the observed inflammatory

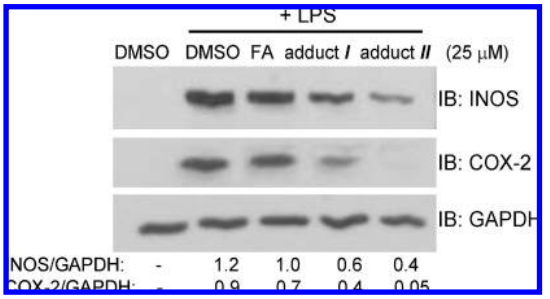

Figure 10. Effect of 25 μM ferulic acid (FA), adduct **I**, and adduct **II** on LPS-induced iNOS and COX-2 expression in RAW 264.7 murine macrophages (representative of $n = 3$).

bioactivity of the phenolic−Maillard reaction products identified in our models may also provide further insights into health benefits of whole grain foods and strategies for process optimization. Future ongoing work in our laboratory is focused on translating the findings of these model systems to whole grain food products in relation to flavor and color development as well as bioactivity. We have tentatively identified similar phenolic−Maillard adduct reaction products in the crust of a whole grain hard red spring wheat bread and hope to report on the chemistry of these products soon.

LITERATURE CITED

(1) Vitaglione, P.; Napolitano, A.; Fogliano, V. Cereal dietary fiber: a natural functional ingredient to deliver phenolic compounds into the gut. *Trends Food Sci. Technol.* **2008**, *19*, 451–463.

(2) Bakke, A.; Vickers, Z. Consumer liking of refined and whole wheat bread. *J. Food Sci.* **2007**, *72*, S473–S480.

(3) Heinio, R. L.; Liukkonen, K. H.; Myllyma, O.; Pihlava, J. M.; Adlercreutz, H.; Heinonen, S. M.; Poutanen, K. Quantities of phenolic compounds and their impacts on the perceived flavour attributes of rye grain. *J. Cereal Sci.* **2008**, *47*, 566–575.

(4) Drewnowski, A. Taste preferences and food intake. *Annu. Rev. Nutr.* **1997**, *17*, 237–253.

(5) Peterson, D. G.; Noda, Y. Role of phenolic reactions on Maillard reaction flavors. In *Recent Highlights in Flavor Chemistry and Biology*, Proceedings of the 8th Wartburg Symposium, Eisenach, Germany, 2007; Hofmann, T., Meyerhof, W., Schieberle, P., Eds.; Deutsche Forschungsanstalt fur Lebensmittelchemie: Eisenach, Germany, 2007; p 443.

(6) Wang, Y. Effects of naturally occurring phenolic compounds on the formation of Maillard aroma. Ph.d. dissertation, Rutgers State University, 2000.

(7) Li, L.; Shewry, P. R.; Ward, J. L. Phenolic acids in wheat varieties in the HEALTHGRAIN diversity screen. *J. Agric. Food Chem.* **2008**, *56*, 9732–9739.

(8) Baynes, J.; Monnier, V.; Ames, J.; Thorpe, S. The Maillard reaction: chemistry at the interface of nutrition, aging, and disease. In *8th International Symposium on the Maillard Reaction*; Baynes, J.,

Monnier, V. M., Ames, J. M., Thorpe, S. R., Eds.; New York Academy of Sciences: Charleston, SC, 2004; Vol. *1043*, p 954.
(9) Friedman, M. Food browning and its prevention: overview. *J. Agric. Food Chem.* **1996**, *44*, 631–653.
(10) Namiki, M. Chemistry of Maillard reactions: recent studies on the browning reaction mechanism and the development of antioxidants and mutagens. *Adv. Food Res.* **1988**, *32*, 115–184.
(11) Schneeman, B. O.; Dunaif, G. Nutritional and gastrointestinal response to heated nonfat dry milk. *J. Agric. Food Chem.* **1984**, *32*, 477–480.
(12) Wakabayashi, K.; Takahashi, M.; Nagao, M.; Sato, S.; Kinae, N.; Tomita, I.; Sugimura, T. Quantification of mutagenic and carcinogenic heterocyclic amines in cooked foods. In *Amino−Carbonyl Reactions in Food and Biological Systems*; Fujimaki, M., Namiki, M., Kato, H., Eds.; Kodansha: Tokyo, Japan, 1986; pp 363−371.
(13) Randhir, R.; Kwon, Y.; Shetty, K. Effects of thermal processing on phenolics, antioxidant activity and health-relvevant functionality of select grain sprouts and seedlings. *Innovative Food Sci. Emerging Technol.* **2008**, *9*, 355–364.
(14) Palempalli, U. D.; Gandhi, U.; Kalantari, P.; Vunta, H.; Arner, R. J.; Narayan, V.; Ravindran, A.; Prabhu, K. S. Gambogic acid covalently modifies IκB-kinase-β subunit to mediate suppression of lipopolysaccharide-induced activation of NF-κB in macrophages. *Biochem. J.* **2009**, *419* (2), 401−409.
(15) Colahan-Sederstrom, P. M.; Peterson, D. G. Inhibition of key aroma compound generated during ultrahigh-temperature processing of bovine milk via epicatechin addition. *J. Agric. Food Chem.* **2005**, *53*, 398–402.
(16) Noda, Y.; Peterson, D. G. Structure−reactivity relationships of flavan-3-ols on product generation in aqueous glucose/glycine model systems. *J. Agric. Food Chem.* **2007**, *55*, 3686–3691.
(17) Schwambach, S. L.; Peterson, D. G. Reduction of stale flavor development in low-heat skim milk powder via epicatechin addition. *J. Agric. Food Chem.* **2006**, *54*, 502–508.
(18) Totlani, V. M.; Peterson, D. G. Reactivity of epicatechin in aqueous glycine and glucose maillard reaction models: quenching of C2, C3, and C4 sugar fragments. *J. Agric. Food Chem.* **2005**, *53*, 4130–4135.
(19) Totlani, V. M.; Peterson, D. G. Epicatechin carbonyl-trapping reactions in aqueous maillard systems: identification and structural elucidation. *J. Agric. Food Chem.* **2006**, *54*, 7311–7318.
(20) Totlani, V. M.; Peterson, D. G. Influence of epicatechin reactions on the mechanisms of Maillard product formation in low moisture model systems. *J. Agric. Food Chem.* **2007**, *55*, 414–420.
(21) Schieberle, P.; Fischer, R.; Hofmann, T. The carbohydrate modul labeling—a useful tool to clarify formation pathways of aroma compounds formed in Maillard-type reactions. In *Flavor Research at the Dawn of the Twenty-First Century*; Le Quéré, J. L., Etiévant, P. X., Eds.; Lavoisier: Paris, France, 2003; pp 447−452.
(22) Benson, L. M.; Naylor, S.; Tomlinson, A. J. Investigation of Maillard reaction products using ^{15}N isotope studies and analysis by electrspray ionization−mass spectrometry. *Food Chem.* **1998**, *62* (2), 179–183.
(23) Stark, T.; Hofmann, T. Application of a molecular sensory science approach to alkalized cocoa (*Theobroma cacao*): structure determination and sensory activity of nonenzymatically C-glycosylated flavan-3-ols. *J. Agric. Food Chem.* **2006**, *54*, 9510–9521.
(24) Snider, B. B. Synthesis of the 5-hydroxymethyl-6-aryl-8-oxabicyclo-[3.2.1]oct-3-en-2-one natural products descurainin and cartorimine. *Tetrahedron* **2006**, *62*, 5171–5177.
(25) Wen, Y.; He, S.; Xue, K.; Cao, F. Studies on chemical constituents of *Ligusticum chuanxiong*. *Chem. Abstr.* **1986**, *105*, 75884m.
(26) Cohen, L. A study of pH dependence in the decarboxylation of *p*-hydroxycinnamic acid. *J. Am. Chem. Soc.* **1959**, *82*, 1907–1911.
(27) Sun, K.; Li, X.; Li, W.; Wang, J.; Liu, J.; Sha, Y. Two new lactones and one new aryl-8-oxa-bicyclo[3,2,1]oct-3-en-2-one from *Descurainia sophia*. *Chem. Pharm. Bull.* **2004**, *52* (12), 1483–1486.
(28) Chuyen, N. V. Studies on the reaction of dipeptides with glyoxal. *Agric. Biol. Chem.* **1973**, *37* (2), 327–334.
(29) Yaylayan, V. A.; Keyhani, A. Glycine specific novel Maillard reaction products: 5-hydroxy-1,3-dimethyl-2(1*H*)-quinoxalinone and related compunds. *J. Agric. Food Chem.* **1997**, *45*, 697–702.
(30) Frank, O.; Blumberg, S.; Kunert, C.; Zehentbauer, G.; Hofmann, T. Structure determination and sensory analysis of bitter-tasting 4-vinylcatechol oligomers and their identification in roasted coffee by means of LC-MS/MS. *J. Agric. Food Chem.* **2007**, *55*, 1945–1954.
(31) Farmar, J.; Ulrich, P.; Cerami, A. Novel pyrroles from sulfite-inhibited Maillard reactions: insight into the mechanism of inhibition. *J. Org. Chem.* **1988**, *53*, 2346–2349.
(32) Bekedam, E. K.; Schols, H. A.; Van Boekel, M. A.; Smit, G. Incorporation of chlorogenic acids in coffee brew melanoidins. *J. Agric. Food Chem.* **2008**, *56*, 2055–2063.
(33) Rizzi, G. P. Free radicals in the Maillard reaction. *Food Rev. Int.* **2003**, *19* (4), 375–395.
(34) Hofmann, T.; Bors, W.; Stettmaier, K. Studies on radical intermediates in the early stage of the nonenzymatic browning reaction of carbohydrates and amino acids. *J. Agric. Food Chem.* **1999**, *47*, 379–390.
(35) Namiki, M.; Hayashi, T. Developments of novel free radicals during the amino−carbonyl reactions of sugars with amino acid. *J. Agric. Food. Chem.* **1975**, *23*, 487–491.
(36) Namiki, M.; Hayashi, T.; Kawakishi, S. Free radicals developed in the amino-carbonyl reaction of sugars with amino acids. *Agric. Biol. Chem.* **1973**, *37*, 2935–2936.
(37) Mitsuda, H.; Yasumoto, K.; Yokoyama, K. Studies on the free radical in amino−carbonyl reaction. *Agric. Biol. Chem.* **1965**, *29*, 751–756.

Received for review March 19, 2009. Revised manuscript received August 7, 2009. Accepted September 10, 2009.